Optimum and Suboptimum Detector Performance for Signals in Cyclostationary Noise

DANIEL BUKOFZER, MEMBER, IEEE

(Invited Paper)

Abstract—**The detection of known and partially known signals in additive white Gaussian nonstationary noise is considered, with primary attention to the case where the time-varying noise intensity parameter $N_0(t)$ is a periodic function. Optimum receiver structures are derived for three detection cases, namely completely known signals, sinusoids with random phase, and sinusoids with both random amplitude and phase. It is demonstrated that optimum receiver performance can be achieved only if proper synchronization to the noise intensity $N_0(t)$ is accomplished. Large performance penalties can be demonstrated when an improperly synchronized receiver is used. Consequently, suboptimum receivers that ignore the noise intensity time variations and therefore require no synchronization, have been considered, and their performance compared to their optimum counterparts. Depending on the type of time-varying noise intensity being considered, results show that performance differences between optimum and suboptimum receivers can be negligible in some cases, and yet can be substantial in other cases. Several examples have been worked out using two different forms for $N_0(t)$ and corresponding performance evaluations have been carried out and presented graphically in terms of receiver error probability as a function of signal-to-noise ratio.**

I. Introduction

A. Purpose

THE well-known theory of detection of known and partially known signals in additive stationary white Gaussian noise [1] is easily extended to detection problems for which the noise is additive, white, and Gaussian, but nonstationary with known time-varying intensity parameter (denoted by $N_0(t)$). If the time variation is periodic, the noise is termed cyclostationary [2], [3]. This type of noise can arise acoustically and electrically from rotating machinery such as electrical motors and generators, reciprocating and turbine engines, and from noise fields containing periodically time-varying inhomogeneities such as rotating or revolving reflectors and refractors. Cyclostationary noise can also arise from intentional electrical interference and from unintentional electrical interference from an information-bearing signal consisting of a modulated periodic carrier. In general, cyclostationary white noise is an idealized model for broad-band noise with periodically varying instantaneous power (intensity). Although some such processes are best modeled as white Poisson impulse noise, only the white Gaussian noise is considered in this paper.

The applicability of a cyclostationary noise model to underwater signal detection problems is due primarily to the following: a) an important source of noise in ships and submarines is self-interference caused by rotating machinery; and b) the ocean medium is most accurately modeled as a time-variant space-variant random filter [4] where the time variation properties may behave in periodic or quasi-periodic fashion.

Optimum detectors for signals in additive white Gaussian cyclostationary noise (denoted by $n(t)$) contain periodically time-varying parameters that must be synchronized to the periodic variation of the noise intensity. This presents two significant practical problems: 1) implementation of appropriately time-varying parameters requires knowledge of the exact waveform of time variation of the noise intensity; and 2) synchronization can be particularly difficult if the observation time is not sufficiently long. A common way to account for the lack of timing information needed for noise synchronization is to model the phase (time reference) of the noise by a random variable that is uniformly distributed over one period (denoted by T) of the time-varying noise intensity. Although this phase randomization stationarizes the noise [5], [6], the optimum detector for the resultant composite detection problem can be too complex for implementation, because phase-randomization does not preserve the Gaussianness of the noise, and optimum detectors for non-Gaussian (particularly continuous-time) noise can be unduly complex. In fact, the nonlinearity that must be implemented (e.g., for the more tractable discrete-time non-Gaussian white noise model [7] cannot be specified without specification of the exact form of time-variation of the noise intensity (before stationarization), because this determines the probability distribution of the stationarized noise.

The preceding difficulties motivate the alternative of modeling the noise by a stationary white Gaussian process (denoted by $\tilde{n}(t)$) having the same time-invariant intensity as the phase randomized (non-Gaussian) white process. This is equivalent to replacing the periodically time-varying intensity parameter in the original cyclostationary white Gaussian model $n(t)$, with its time-averaged value defined by

$$\langle N_o \rangle \triangleq \frac{1}{T}\int_0^T N_o(t)\,dt. \tag{1}$$

Thus the time-varying impulsive autocorrelation of $n(t)$

$$E\{n(t+\tau)n(t)\} = N_o(t)\delta(\tau) \tag{2}$$

is in effect, replaced with the time-invariant impulsive autocorrelation

$$E\{\tilde{n}(t+\tau)\tilde{n}(t)\} = \langle N_o \rangle \delta(\tau). \tag{3}$$

Manuscript received April 7, 1986; revised August 27, 1986.
The author is with the Naval Postgraduate School, Monterey, CA 93943.
IEEE Log Number 8714262.

Since the probability distribution of $\tilde{n}(t)$ is assumed to be Gaussian, the simplicity of the optimum detector for Gaussian noise is retained, but the periodically time-varying parameters and the synchronizer are circumvented.

The purpose of this paper is to evaluate this approach to detector design, by evaluating and comparing the probabilities of detection error for the potentially impractical optimum noise-synchronized periodically time-varying detector, and the practical suboptimum time-invariant detector (that is optimum for the modified model $\tilde{n}$, of the actual noise n). This is carried out for three types of signals: arbitrary sure signals, sinusoidal signals with random phase, and sinusoidal signals with random amplitude and random phase.

Although only cyclostationary noise is considered in this paper, the general approach to suboptimum detector design, and the methods of analysis of performance are applicable to nonstationary white Gaussian noise that is not necessarily cyclostationary.

B. Optimum and Suboptimum Detectors

The signal detection problems addressed in this paper are modeled in the conventional way as hypothesis testing problems. Under each of two hypotheses (denoted by H_1 and H_0), the received waveform (denoted by $r(t)$) consists of a signal ($s_1(t)$ under H_1 and $s_0(t)$ under H_0) in additive white Gaussian noise (denoted by $n(t)$):

$$\begin{aligned} H_1 &: r(t)=s_1(t)+n(t) \\ H_0 &: r(t)=s_0(t)+n(t) \end{aligned} \qquad t \in T_0 \tag{4}$$

where T_0 is the time interval of observation of $r(t)$. To determine the optimum detector, the cyclostationary white Gaussian noise with time-varying intensity $N_o(t)$ is converted to stationary white Gaussian noise with time-invariant intensity $\langle N_o \rangle$ by multiplying the observed waveform $r(t)$ by the known time-varying factor $[\langle N_o \rangle / N_o(t)]^{1/2}$. (It is assumed that $N_o(t) \neq 0$.) This yields the equivalent hypothesis testing problem:

$$\begin{aligned} H_1 &: \tilde{r}(t)=\tilde{s}_1(t)+\tilde{n}(t) \\ H_0 &: \tilde{r}(t)=\tilde{s}_0(t)+\tilde{n}(t) \end{aligned} \qquad t \in T_0 \tag{5}$$

where $\tilde{r}(t)$ is defined by

$$\tilde{r}(t)=[\langle N_o \rangle / N_o(t)]^{1/2} r(t) \tag{6}$$

and $\tilde{s}_1(t)$, $\tilde{s}_0(t)$, $\tilde{n}(t)$ are similarly defined. Problems (4) and (5) are equivalent because (6) is an invertible transformation. Therefore, conventional methods [1] for determining optimum detectors for known signals in white Gaussian stationary noise can be applied to problem (5) to solve problem (4).

To determine the suboptimum detector (that is, not time-varying or noise-synchronized), the hypothesis testing problem (4) is modified to

$$\begin{aligned} H_1 &: r(t)=s_1(t)+\tilde{n}(t) \\ H_0 &: r(t)=s_0(t)+\tilde{n}(t) \end{aligned} \qquad t \in T_0. \tag{7}$$

Since the only difference between (4) and (7) is that the time-varying parameter $N_o(t)$ in (4) is replaced with the time-invariant parameter $\langle N_o \rangle$ (cf. (1)–(3)), then the optimum detector obtained from (5) for (4) yields the optimum detector for (7) (which is the suboptimum detector for (4)) simply by replacement of $N_o(t)$ with $\langle N_o \rangle$ in the formulas that specify the optimum detector for (4).

In this paper, the Bayes' optimization criterion of minimum risk is adopted. Therefore, the optimum detector will be (equivalent to) a likelihood ratio test. For each of the specific detection problems considered in Sections II–IV, the log likelihood ratio takes the form

$$Z[\{r(t) : t \in T_0\}] \underset{H_0}{\overset{H_1}{\gtrless}} \gamma \tag{8}$$

where $Z[\{r(t): t \in T_0\}]$ is a sufficient statistic, which depends on $N_o(t)$, and the threshold level γ which consists of two additive terms, one of which is determined by decision costs and prior probabilities of H_0 and H_1, and the other of which depends on signal energies and noise intensity $N_o(t)$. Thus both the sufficient statistic $Z[\{r(t): t \in T_0\}]$ and the threshold level γ are modified by replacement of $N_o(t)$ with $\langle N_o \rangle$ to obtain the suboptimum detector from the optimum.

For notational convenience, we introduce the abbreviated notation

$$q(t) \triangleq [N_0(t)/\langle N_0 \rangle]^{1/2}$$

for the noise stationarizing factor (6).

II. Detection of Known Signals

For the problem of detection of known signals, $s_1(t)$ and $s_0(t)$ (i.e., discrimination between $s_1(t)$ and $s_0(t)$), the optimum detector for (4) is given by (8) with

$$Z[\{r(t)\}] \triangleq \int_{T_0} \{[s_1(t)-s_0(t)]/q(t)\} r(t)\, dt \tag{9}$$

$$\gamma \triangleq \langle N_0 \rangle \ln(\lambda) + \int_{T_0} \{[s_1^2(t)-s_0^2(t)]/q(t)\}\, dt \tag{10}$$

where λ is determined solely by decision costs and prior probabilities [1, (12), p. 26]. Equation (9) describes the conventional correlator (or matched filter) detector preceded by the periodically time-varying scale factor $1/q(t)$, which is synchronized to the cyclostationary noise with intensity $q^2(t) \cdot \langle N_o \rangle$. A diagram of the detector structure is shown in Fig. 1. The probability of detection error is [1, (69a), p. 37]

$$P_e = \frac{p_1}{\sqrt{2\pi}} \int_{-\infty}^{a_-} e^{-x^2/2}\, dx + \frac{1-p_1}{\sqrt{2\pi}} \int_{a_+}^{\infty} e^{-x^2/2}\, dx \tag{11}$$

where p_1 is the prior probability, $p_1 = P[H_1]$, and

$$a_\pm \triangleq \frac{\langle N_o \rangle \ln(\lambda) \pm E_q(1-R_q)}{[2\langle N_o \rangle E_q(1-R_q)]^{1/2}} \tag{12}$$

$$E_q \triangleq \frac{1}{2} \int_{T_0} \{[s_0^2(t)+s_1^2(t)]/q(t)\}\, dt \tag{13}$$

$$R_q \triangleq \int_{T_0} \{s_0(t)s_1(t)/q(t)\}\, dt. \tag{14}$$

For the special case of equal priors and costs, $\lambda = 1$ and

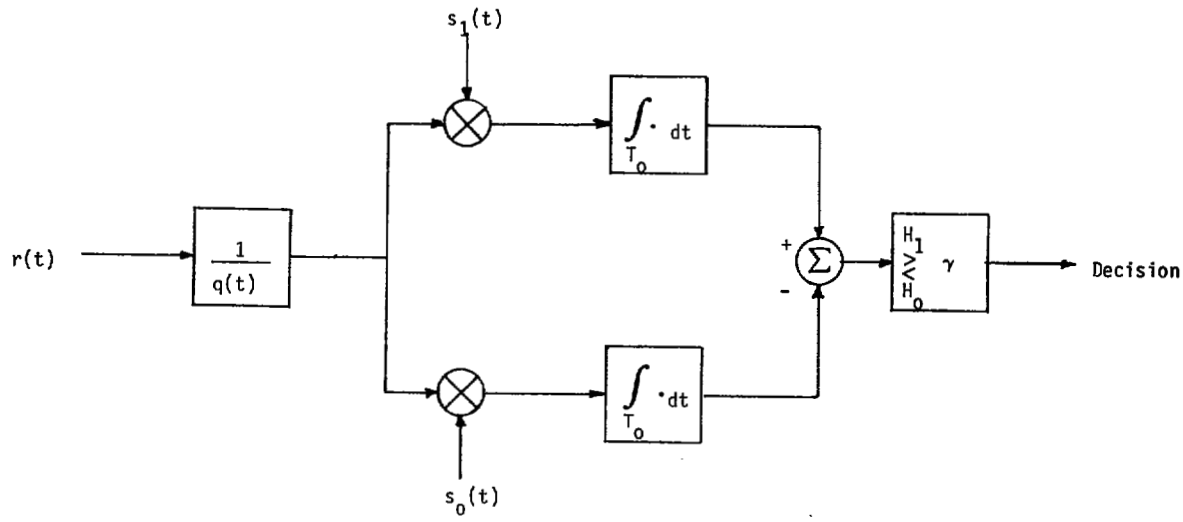

Fig. 1. Optimum receiver for known signals.

$$P_e = \text{erfc}\ \{[(1-R_q)E_q/2\langle N_o\rangle]^{1/2}\} \tag{15}$$

where erfc $\{\cdot\}$ is the complementary error function [1, (66), p. 37] defined by

$$\text{erfc}\ \{a\} = \frac{1}{\sqrt{2\pi}} \int_a^\infty e^{-x^2/2}\, dx.$$

Letting $\rho_q = 2(1 - R_q)E_q/\langle N_o\rangle$, (15) takes on the form

$$P_e = \text{erfc}\ \{[\rho_q/4]^{1/2}\}.$$

The suboptimum detector for (4) (optimum detector for (7)) is given by (8)–(10) with $N_o(t)$ replaced with $\langle N_o\rangle$, which is equivalent to replacing $q(t)$ with 1. The structure of this detector is identical to that shown in Fig. 1 except for replacement of $q(t)$ by 1. The probability of error (which is denoted by $\tilde{P}_e$) that results from using this suboptimum detector with the cyclostationary noise can be shown to be given by (11) with $a_\pm$ replaced by

$$\tilde{a}_\pm \triangleq \frac{\langle N_o\rangle \ln(\lambda) \pm E(1-R)}{[2J\langle N_o\rangle E(1-R)]^{1/2}} \tag{16}$$

where E and R are defined by (13) and (14) with $q(t)$ replaced by 1, and

$$J \triangleq \int_{T_0} [s_1(t)-s_0(t)]^2 q(t)\, dt \Big/ \int_{T_0} [s_1(\tau)-s_0(\tau)]^2\, d\tau. \tag{17}$$

For the special case of equal priors and costs, $\lambda = 1$ and

$$\tilde{P}_e = \text{erfc}\ \{[(1-R)E/2\langle N_o\rangle J]^{1/2}\}. \tag{18}$$

Observe that if the noise were stationary, then $J = 1$; therefore, J is a factor related to the amount by which the signal-to-noise ratio (SNR), which is defined by

$$\rho \triangleq 2(1-R)E/\langle N_o\rangle$$

is effectively reduced or increased when cyclostationary noise enters a detector intended for stationary noise. However, J is not the amount by which the SNR must be boosted to make the suboptimum receiver perform as well as the optimum receiver for cyclostationary noise. Rather, comparison of (15) and (18) reveals that $P_e = \tilde{P}_e$ if and only if the SNR is boosted by the factor

$$D \triangleq J(1-R_q)E_q/(1-R)E = J\rho_q/\rho. \tag{19}$$

This factor D can be interpreted as an effective SNR degradation factor. In terms of the SNR ρ, (18) becomes

$$\tilde{P}_e = \text{erfc}\ \{[\rho/4J]^{1/2}\}.$$

The performance parameters ρ, J, D can be reinterpreted in terms of distances between signals as follows. We let d_q denote the weighted distance between $s_1(t)$ and $s_0(t)$:

$$d_q \triangleq \left[\int_{T_0} \{[s_1(t)-s_0(t)]^2 q(t)\}\, dt\right]^{1/2}$$

with weight function $q(t)$. Then we obtain

$$\rho = d_1^2/2\langle N_o\rangle$$

$$J = d_q^2/d_1^2$$

$$D = d_q^2 d_{1/q}^2/d_1^4.$$

From the Cauchy–Bunyakovski–Schwartz (CBS) inequality

$$\left[\int_{T_0} [s_1(t)-s_0(t)]^2\, dt\right] \le \int_{T_0} [s_1(t)-s_0(t)]^2 q(t)\, dt \cdot \int_{T_0} [s_1(t)-s_0(t)]^2 \frac{1}{q(t)}\, dt$$

so that

$$d_1^4 \le d_q^2 d_{1/q}^2$$

thus confirming that the suboptimum detector requires a higher SNR than the optimum detector if the former is to perform as well as the latter (i.e., $D \ge 1$).

Example 1:

Consider the on–off signaling scheme for which

$$s_0(t) \equiv 0$$

$$s_1(t) = A \sin (2\pi Mt/T) \tag{20}$$

and $T_0 = [0, NT]$, where M and N are positive integers. Consider also a square-wave periodic noise intensity that is defined over one period by

$$N_o(t) = \begin{cases} \langle N_o \rangle b & 0 \le t \le cT \\ \langle N_o \rangle ab & cT < t \le T \end{cases} \tag{21}$$

where

$$b \triangleq (c + a - ac)^{-1}$$

which insures that (21) is self-consistent, and

$$0 < a,\ c \le 1.$$

Then $R_q = R = 0$, and

$$E = NTA^2/4 = T_0A^2/4 \tag{22}$$

$$E_q = (E/b)\{c + (1-c)/a + [(1-a)/4\pi Mc] \sin (4\pi Mc)\} \tag{23}$$

$$J = 1 - [b(c - ac)/4\pi Mc] \sin (4\pi Mc). \tag{24}$$

Therefore, (19) yields

$$D = (1/a)\{ac + 1 - c + [c(1-a)/4\pi Mc] \sin (4\pi Mc)\} \cdot \{b^{-1} - [c(1-a)/4\pi Mc] \sin (4\pi Mc)\}. \tag{25}$$

For a time-symmetric square wave, $c = 1/2$ and D simplifies to

$$D = (1 + a)^2/4a \tag{26}$$

which can be very large if a is small. This is to be expected since the optimum noise-synchronized detector can exploit low-noise (small a) intervals of time, but the suboptimum time-invariant detector cannot. In contrast, if $c \simeq 1$, $(1 - c \ll a)$, then $D \simeq 1$, as expected since the cyclostationary noise is nearly stationary in this case in the sense that the periodic noise intensity of (21) is very nearly equal to the constant level $\langle N_o \rangle$ for almost its entire period. The same result holds true for small values of c, $(c \ll 1/M)$.

It follows from (15), (18), (19), (22)–(24), and $R = R_q = 0$ that

$$P_e = \text{erfc } \{(D\rho/4)^{1/2}\} \tag{27}$$

$$\tilde{P}_e = \text{erfc } \{(\rho/4)^{1/2}\} \tag{28}$$

where D is given by (25). Graphs of P_e and $\tilde{P}_e$ as functions of SNR, ρ, for several values of the parameters a and c (which control the degree of nonstationarity of the noise) are shown in Figs. 2 and 3. Note that for values of c (such as 1/4 or 3/4) causing $4Mc$ to be an integer, D becomes

$$D = \frac{(a-1)^2c(1-c) + a}{a}. \tag{29}$$

If we compare this expression for D with (26) (for which $c = 1/2$), we see that

$$\frac{(a-1)^2c(1-c) + a}{a} \ll \frac{(1+a)^2}{4a}$$

whenever $c \ll 1$. This implies that P_e (given by (27)) is considerably larger for small values of c (with $4Mc$ an integer) in comparison to P_e for the symmetric wave case ($c = 1/2$).

Example 2:

Consider again the on–off signaling scheme (20), but with a sinusoidal periodic noise intensity that is defined by

$$N_o(t) = b\langle N_o \rangle [1 + a - (1-a) \cos (2\pi t/T)] \tag{30}$$

where

$$b \triangleq (1 + a)^{-1}$$

which insures that (30) is self-consistent, and

$$0 < a \le 1.$$

Then $R_q = R = 0$ and

$$E = NA^2/2(1 + a) \tag{31}$$

$$J = 1 \tag{32}$$

and use of the identity (for $\beta < 1$) [8]

$$\frac{1}{2\pi} \int_0^{2\pi} \frac{\cos \alpha t}{1 + \beta \cos t}\, dt = (-\upsilon)^{\alpha} \frac{(1 + \upsilon^2)}{(1 - \upsilon^2)}$$

where

$$\upsilon \triangleq \beta/[1 + (1 - \beta^2)^{1/2}]$$

yields

$$E_q = E(1 + d)(1 - d^M)/(1 - d) \tag{33}$$

for which

$$d \triangleq (1-a)^2/(1 + a + 2\sqrt{a})^2 < 1.$$

Therefore, (19) yields

$$D = (1 + d)(1 - d^M)/(1 - d). \tag{34}$$

For high-frequency signals ($M \gg 1$), (34) reduces to

$$D \simeq (1 + d)/(1 - d) \tag{35}$$

which can be very large if a is small. However, D in (35) does not grow as fast with decreasing a as D in (26) because the low-noise time intervals of the sinusoidal noise intensity (30) are of shorter duration than those of the square wave noise intensity.

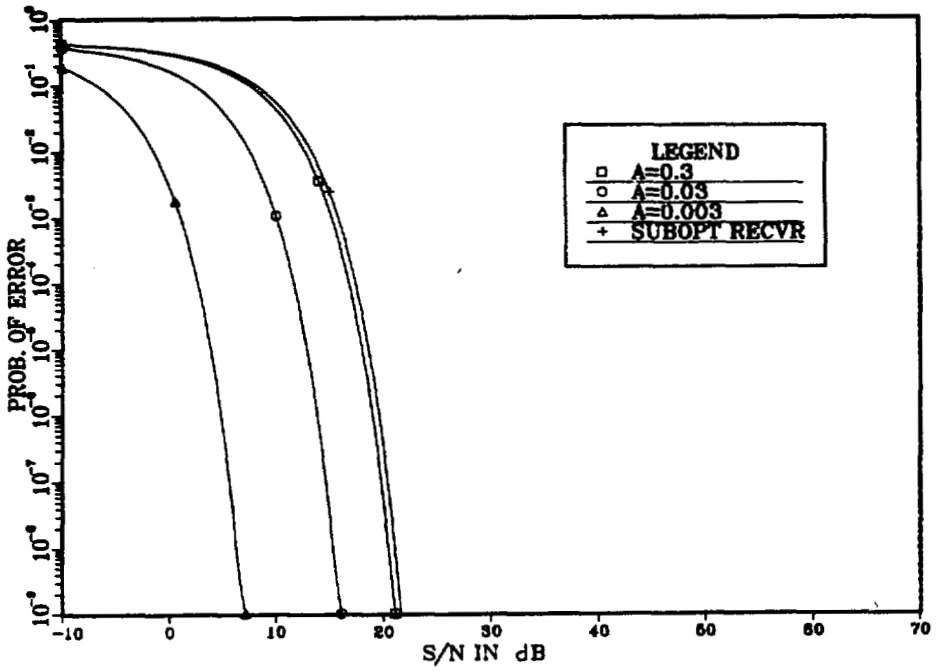

Fig. 2. Receiver performance for Example 1 with nonsymmetric noise intensity factor.

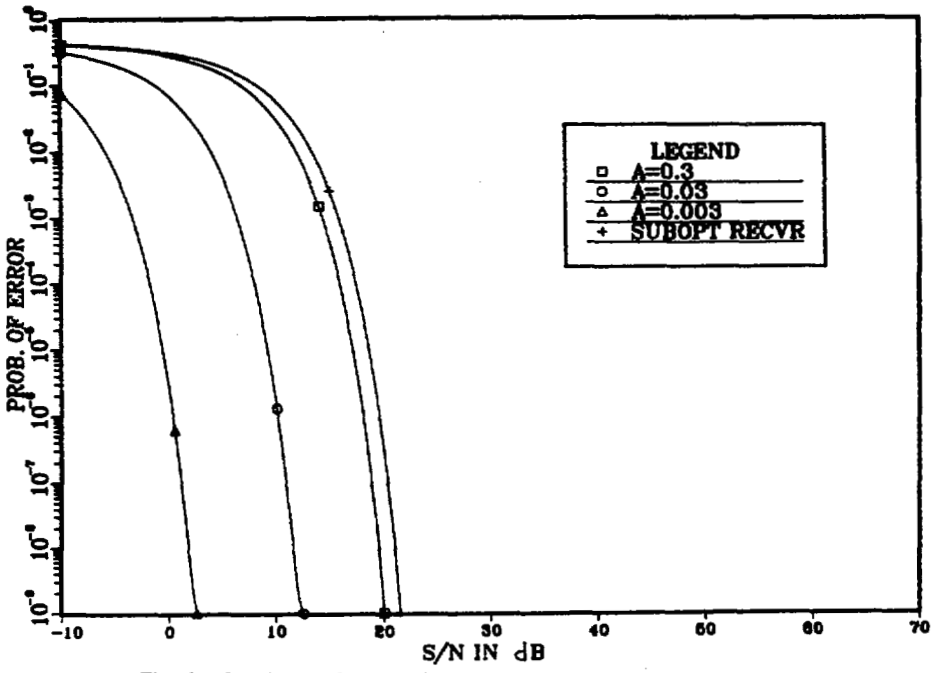

Fig. 3. Receiver performance for Example 1 with symmetric noise intensity factor.

It follows from (15), (18), (19), (31)–(33), and $R = R_q = 0$, that P_e and P_e are given by (28) and (29), where D is given by (34). Graphs of P_e and $\tilde{P}_e$ are shown in Fig. 4.

Penalty Due to Missynchronization

In practice, the SNR degradation incurred through use of the suboptimum time-invariant detector should be weighed against effective SNR degradation due to missynchronization of the optimum time-varying detector. It can be shown that the probability of error (denoted by $\hat{P}_e$) that results from using an incorrect periodic scale factor (denoted by $\hat{q}(t)$) instead of the correct factor $q(t)$ in the detector (9) is given by (11) with $a_\pm$ replaced by

$$\hat{a}_\pm \triangleq \frac{\langle N_0 \rangle \ln(\lambda) \pm E_{\hat{q}}(1 - R_{\hat{q}})}{[2\tilde{J}\langle N_o \rangle E_{\hat{q}}(1 - R_{\hat{q}})]^{1/2}} \tag{36}$$

where $E_{\hat{q}}$ and $R_{\hat{q}}$ are defined by (13) and (14) with $q(t)$

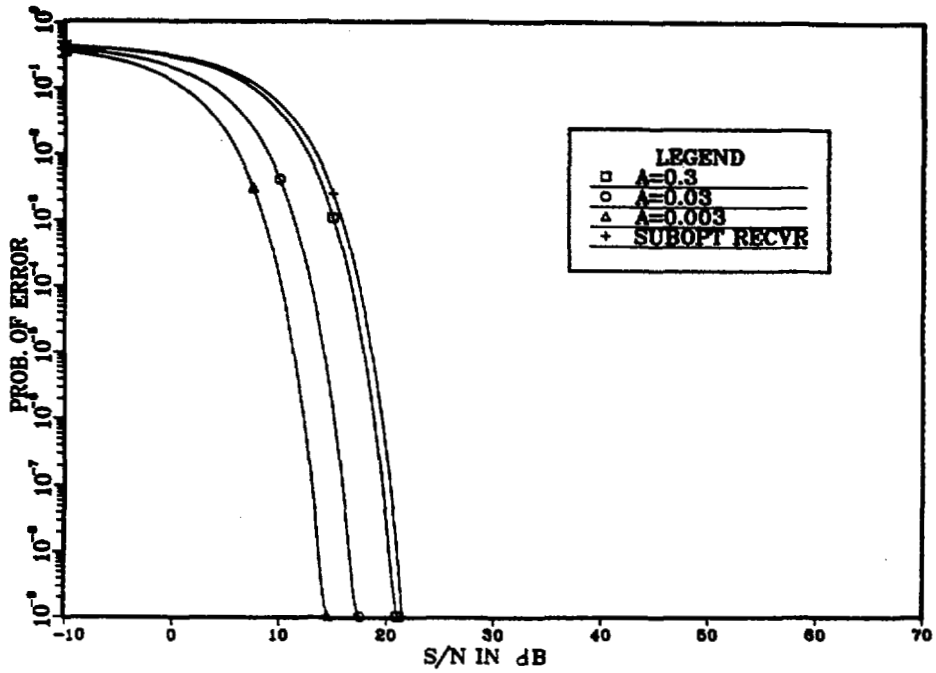

Fig. 4. Receiver performance for Example 2.

replaced by $\hat{q}(t)$, and

$$\hat{J} \triangleq \int_{T_0} \frac{q(t)}{\hat{q}^2(t)} [s_1(t)+s_0(t)]^2\, dt \Big/ \int_{T_0} \frac{[s_1(\tau)-s_0(\tau)]^2}{\hat{q}(\tau)}\, d\tau$$

$$= d^2_{q/\hat{q}^2}/d^2_{1/\hat{q}}. \tag{37}$$

For the special case of equal priors and costs, $\lambda = 1$ and

$$\hat{P}_e = \text{erfc}\ \{[(1-R_{\hat{q}})E_{\hat{q}}/2\langle N_o\rangle \hat{J}]^{1/2}\}$$
$$= \text{erfc}\ \{d^2_{1/\hat{q}}/2d_{q/\hat{q}^2}\langle N_o\rangle^{1/2}\}. \tag{38}$$

Observe that if the correct scaling waveform $q(t)$ were used in the detector, then $\hat{J} = 1$; therefore, $\hat{J}$ is the factor by which SNR is effectively reduced or increased when one cyclostationary noise (with intensity $q(t)$) enters a detector intended for another cyclostationary noise (with intensity $\hat{q}(t)$). However, $\hat{J}$ is not the amount by which SNR must be boosted to make the missynchronized detector perform as well as the correctly synchronized detector. Rather, comparison of (15) and (38) reveals that $P_e = \hat{P}_e$ if and only if SNR is boosted by the factor

$$\hat{D} = \hat{J}(1-R_q)E_q/(1-R_{\hat{q}})E_{\hat{q}} = \hat{J}_{\rho_q}/\hat{\rho} = d^2_{1/q}d^2_{q/\hat{q}^2}/d^4_{1/\hat{q}} \geq 1 \tag{39}$$

where

$$\hat{\rho} = 2(1-R_{\hat{q}})E_{\hat{q}}/\langle N_o\rangle.$$

Thus

$$\hat{P}_e = \text{erfc}\ \{[\hat{\rho}/4\hat{J}]^{1/2}\} = \text{erfc}\ \{[\rho_q/4\hat{D}]^{1/2}\}. \tag{40}$$

Example 1 Continued:

The on–off signaling scheme given by (20) with noise having characteristics given by (21) is analyzed here under the assumption that the optimum receiver is missynchronized. We model this missynchronization by letting

$$\hat{q}(t) = q(t+\epsilon T/2), \qquad 0 \leq \epsilon \leq 1 \tag{41}$$

and for analytical simplicity, we set $c = 1/2$, so that

$$N_o(t) = \begin{cases} \langle N_0\rangle \dfrac{2}{1+a}, & 0 \leq t \leq T/2 \\ \langle N_0\rangle \dfrac{2a}{1+a}, & T/2 < t \leq T. \end{cases} \tag{42}$$

After some algebraic manipulation, we obtain

$$d^2_{1/\hat{q}} = \frac{T_0A^2(1+a)^2}{8a} \tag{43}$$

$$d^2_{q/\hat{q}^2} = \frac{T_0A^2(1+a)}{8}\left[(1-\epsilon)+\epsilon\ \sin\ cM\epsilon + \frac{1}{a^2}\{\epsilon-\epsilon\ \sin\ cM\epsilon\} + \frac{1}{a}\{(1-\epsilon) + \sin\ cM\epsilon\} + a\{\epsilon-\epsilon\ \sin\ cM\epsilon\}\right]. \tag{44}$$

From (23) we have (with $c = 1/2$)

$$d^2_{1/q} = T_0A^2(1+a)^2/8a. \tag{45}$$

Equations (43)–(45) can now be used in (38) and (39) in order to express $\hat{P}_e$ and $\hat{D}$ as functions of ϵ, the measure of missynchronization. Thus

$$\hat{P}_e = \text{erfc}\left\{\left[\frac{T_0A^2(1+a)^3}{32a^2g(\epsilon)\langle N_o\rangle}\right]^{1/2}\right\}$$

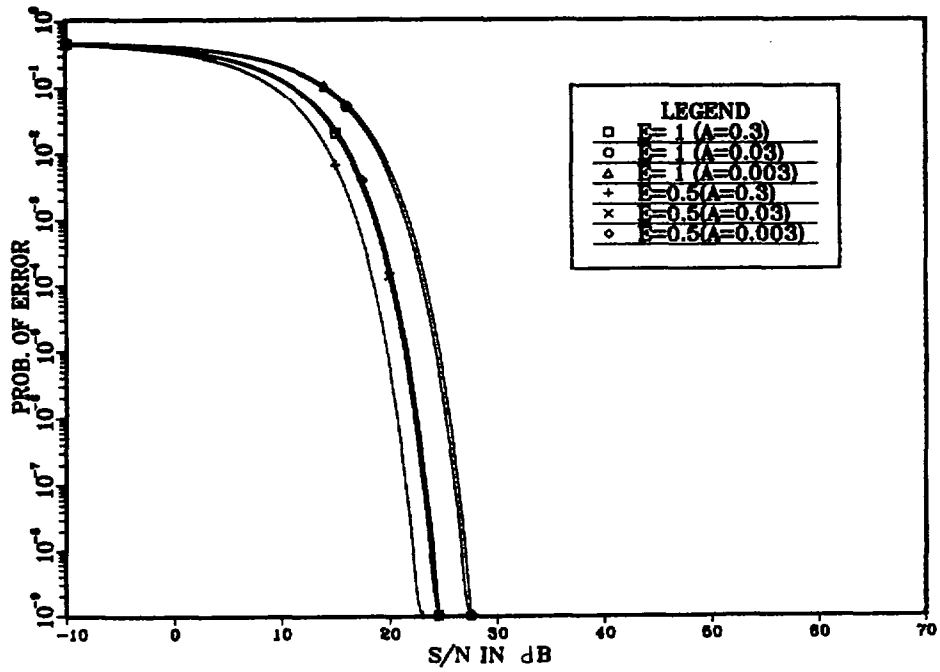

Fig. 5. Receiver performance for Example 1 with 50- and 100-percent missynchronization.

where

$$g(\epsilon)=(1-\epsilon)+\epsilon \sin cM\epsilon + a^{-2}[\epsilon-\epsilon \sin cM\epsilon] + a^{-1}[(1-\epsilon)+\epsilon \sin cM\epsilon]+a[\epsilon-\epsilon \sin cM\epsilon].$$

Also

$$\hat{D}=\frac{ag(\epsilon)}{(1+a)}.$$

The complicated form of these expressions does not allow a qualitative analysis of performance for arbitrary values of ϵ. For $a = 1$, however, $\hat{P}_e = P_e = \tilde{P}_e$ and $\hat{D} = 1$ as must be the case. A worst-case analysis is undertaken where ϵ is set to the value 1, representing the greatest amount of missynchronization in the receiver. Then $g(\epsilon) = a + a^{-2}$ and

$$\hat{P}_e=\text{erfc}\left\{\left[\frac{T_0A^2(1+a)^3}{32\langle N_o\rangle(1+a^3)}\right]^{1/2}\right\}$$

$$=\text{erfc}\left\{\left(\frac{\rho}{4}\right)^{1/2}\sqrt{\frac{(1-a)^3}{4(1+a^3)}}\right\} \quad (46)$$

$$D=(1+a^3)/a(1+a). \quad (47)$$

Comparison of (46) with (28) reveals that the completely missynchronized receiver ($\epsilon = 1$) has larger probability of error than the suboptimum (unsynchronized) detector, since $\sqrt{(1+a)^3/4(1+a^3)} \leq 1$ for $0 < a \leq 1$. Also from (47) it can be seen that for small values of a, the missynchronized detector requires a larger SNR boost than that required by the suboptimum detector in order for it to perform as well as the properly synchronized detector. For 50-percent missynchronization ($\epsilon = 1/2$)

$$\hat{P}_e=\text{erfc}\left\{\left(\frac{\rho}{4}\right)^{1/2}\sqrt{\frac{(1+a)^2}{2(1+a^2)}}\right\}$$

and since $\sqrt{(1+a)^2/2(1+a^2)} \leq 1$ for $0 < a \leq 1$, it is clear that this detector has inferior performance in comparison to the suboptimum (unsynchronized) detector, yet since $\sqrt{(1+a)^2/2(1+a^2)} \geq \sqrt{(1+a)^3/4(1+a^3)}$ for $0 < a \leq 1$, the performance of the 50-percent missynchronized detector is, of course, better than that of the completely missynchronized detector, with the greatest difference occurring as $a \to 0$. (In the limit, this is equivalent to a 1.5 dB SNR difference between the two missynchronized detectors.)

Graphs of $\hat{P}_e$ for 50- and 100-percent missynchronization are shown in Fig. 5. This example demonstrates that achievement of synchronization is important for the proper performance of the optimum detector. If synchronization is difficult to achieve, it may be more appropriate to implement the simpler suboptimum detector for which synchronization is not required. The graphs of the ratios $\hat{P}_e/P_e$, $\tilde{P}_e/P_e$, and $\hat{P}_e/\tilde{P}_e$ shown in Fig. 6 for 100-percent missynchronization serve to further highlight this point.

III. Detection of a Sinusoid with Random Phase

The signal detection problem addressed in this section is modeled in the conventional way as a hypothesis testing problem (see (4)), with

$$s_1(t)=s(t,\theta)=A \sin\left[\frac{2\pi Mt}{T}+\theta\right] \quad (48)$$

$$s_0(t) \equiv 0$$

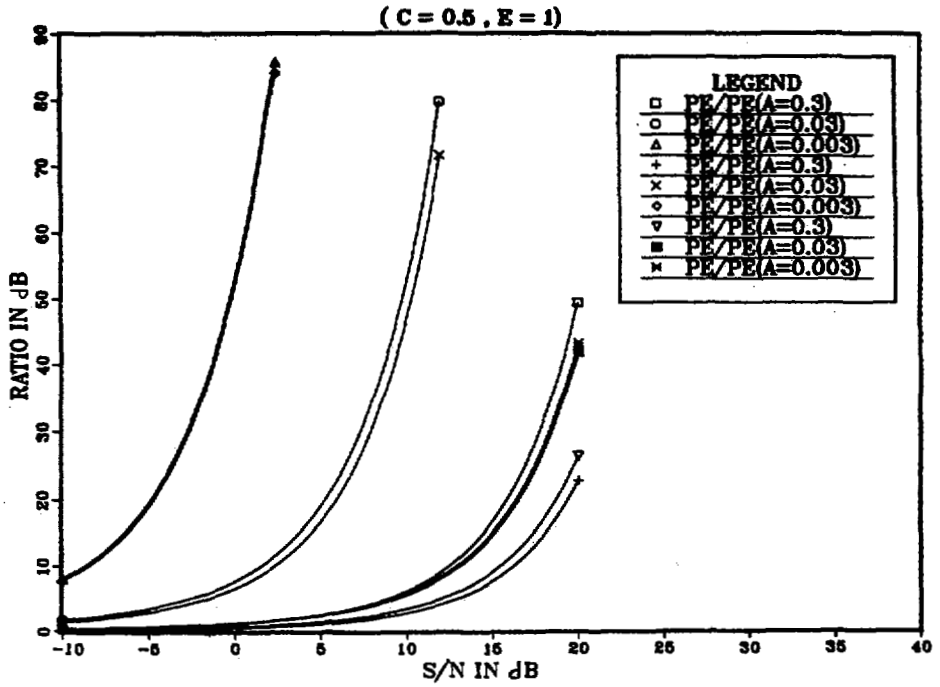

Fig. 6. Performance comparisons of optimum, suboptimum, and 100-percent missynchronized reviewers for Example 1.

and θ is a random variable with pdf $P_\Theta(\theta)$ that is uniform over $[0, 2\pi]$. The optimum detector for (4) and (48), is given by (8) with (see [9])

$$Z[\{r(t)\}] \triangleq \frac{1}{2\pi}\int_0^{2\pi} \exp\left\{\frac{1}{\langle N_o\rangle}\int_{T_0}\frac{s(t,\alpha)}{q(t)}r(t)\,dt\right\} d\alpha \quad (49)$$

$$\gamma = \lambda \exp\left\{\frac{1}{2\langle N_o\rangle}\int_{T_0}\frac{s^2(t,\alpha)}{q(t)}\,dt\right\}. \quad (50)$$

Derivation of (49) and (50) is based on the assumption that $T_0 \gg T$ so that the integral

$$\int_{T_0}\frac{s^2(t,\theta)}{q(t)}\,dt \triangleq k(\theta) \quad (51)$$

is approximately independent of θ. If $T_0 = NT$, N an integer, then $k(\theta)$ is independent of θ, regardless of size of N, provided that

$$\bar{q}_{2M} = \bar{q}_{-2M} = 0 \quad (52)$$

where $\{\bar{q}_i\}$ is the set of Fourier coefficients resulting from an exponential Fourier series expansion of the periodic factor $1/q(t)$. This is due to the fact that

$$k(\theta) = \int_0^{NT}\frac{A^2}{2q(t)}\,dt - \frac{A^2}{2} \cdot \int_0^{NT}\sum_{i=-\infty}^{\infty}\bar{q}_i e^{j2\pi it/T}\cos\left(\frac{4\pi Mt}{T}+2\theta\right)dt$$

where the second integral is directly proportional to the sum $\bar{q}_{2M} + \bar{q}_{-2M}$. For instance, when $q(t)$ is given by (21) in Example 1 (after division by $\langle N_o\rangle$) we have

$$\bar{q}_i = \frac{1}{T}\int_0^{cT}\frac{1}{b}e^{-j2\pi it/T}\,dt + \frac{1}{T}\int_{cT}^{T}\frac{1}{ab}e^{-j2\pi it/T}\,dt$$
$$= \frac{c(c+a)(a-1)}{a}\frac{\sin \pi ic}{\pi ic}e^{-j\pi ic}.$$

Clearly $\bar{q}_{2M} = \bar{q}_{-2M} = 0$ whenever $2Mc$ is a nonzero integer. For $q(t)$ given by (30) in Example 2 (after division by $\langle N_o\rangle$), we obtain

$$\bar{q}_i = \frac{1}{T}\int_{-T/2}^{T/2}\frac{\cos 2\pi it/T}{b[1+a-(1-a)\cos 2\pi t/T]}\,dt$$
$$= \left[\frac{1-a}{a+1+2\sqrt{a}}\right]^i \frac{(a+1+2\sqrt{a})^2+(a-1)^2}{(a+1+2\sqrt{a})^2-(a-1)^2}.$$

Since the term in brackets never exceeds 1 or $0 < a \le 1$, then $\bar{q}_{2M} = \bar{q}_{-2M}$ becomes negligibly small for M large enough. Note, however, that when $a \ll 1$, increasingly large values of M are required to make the terms $\bar{q}_{2M}$ and $\bar{q}_{-2M}$ insignificant.

Equation (49) describes the conventional quadrature correlator receiver preceded by the periodically time-varying factor $1/q(t)$, which is synchronized to the cyclostationary noise with intensity $q^2(t)\cdot\langle N_o\rangle$. The structure of this detector is shown in Fig. 7. This result follows the fact that (49) can be reexpressed in terms of $I_0(\cdot)$, the modified Bessel function. That is:

$$Z[\{r(t)\}] = I_0(Ap/\langle N_o\rangle) \quad (53)$$

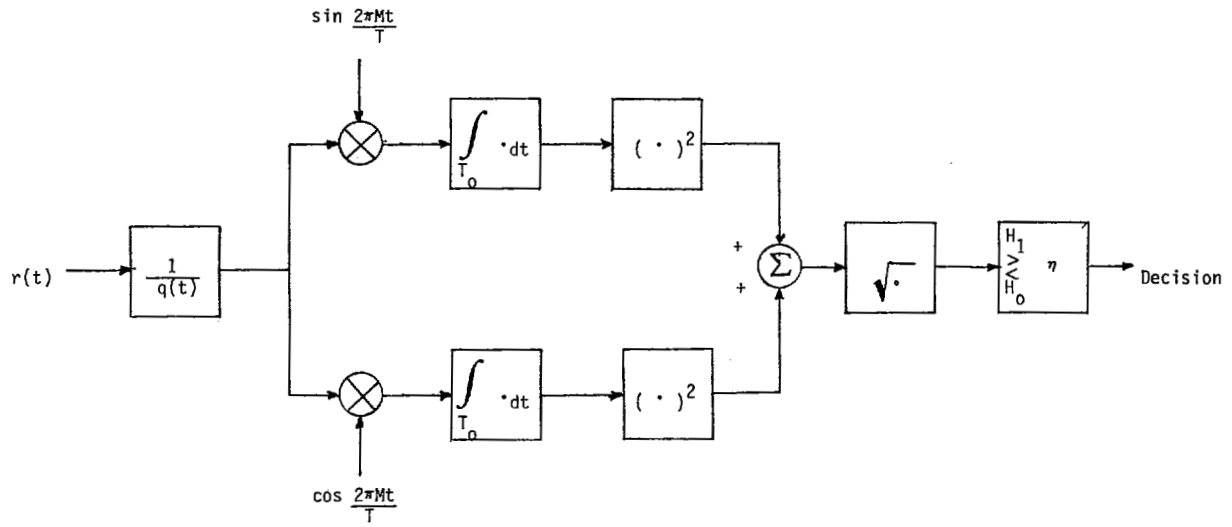

Fig. 7. Optimum receiver for sinusoidal signals having random phase.

where

$$p^2=\left[\int_{T_0}\frac{1}{q(t)}\sin\frac{2\pi Mt}{T}\,r(t)\,dt\right]^2+\left[\int_{T_0}\frac{1}{q(t)}\cos\frac{2\pi Mt}{T}\,r(t)\,dt\right]^2\triangleq y^2+x^2. \quad (54)$$

Note that the receiver need not evaluate $I_0(Ap/\langle N_o\rangle)$ and compare it to γ. Since $I_0(\cdot)$ is a monotonic function, the receiver need only evaluate p^2 and compare it with a new threshold η^2, where η is the value of p for which $I_0(Ap/\langle N_o\rangle) = \gamma$.

The probability of detection error is given by [9, p. 204]

$$P_e=\frac{1}{2}\left[e^{-b^2/2}+\int_b^\infty v\exp\left\{\frac{v^2+\Omega^2}{-2}\right\}I_0(\Omega v)\,dv\right] \quad (55)$$

where

$$b=\eta/\sqrt{\text{var}\,\{X/\theta,\,H_1\}}$$
$$\Omega^2=A^2\,\text{var}\,\{X/\theta,\,H_1\}/\langle N_o\rangle^2. \quad (56)$$

This expression for P_e is derived assuming that $P\{H_1\} = 1/2$, and that

$$\sigma_T^2\triangleq\text{var}\,\{X/\theta,\,H_1\}=\langle N_o\rangle\int_{T_0}\frac{\cos^2 2\pi Mt/T}{q(t)}\,dt$$
$$\equiv\langle N_o\rangle\int_{T_0}\frac{\sin^2 2\pi Mt/T}{q(t)}\,dt$$
$$=\text{var}\,\{Y/\theta,\,H_1\}$$

with the additional constraint that

$$E\{[X-E\{X\}][Y-E\{Y\}]/\theta,\,H_1\}=\frac{\langle N_o\rangle}{2}\int_{T_0}\frac{\sin 4\pi Mt/T}{q(t)}\,dt\equiv 0 \quad (57)$$

where X and Y are defined in (54). Any $q(t)$ for which $\bar{q}_{2M} = \bar{q}_{-2M} = 0$ will satisfy these conditions. Thus the factor $q(t)$ of Example 1 (under the symmetric conditions $c = 1/2$) satisfies the above requirements. The factor $q(t)$ of Example 2 was shown to have $\bar{q}_{\pm 2M} \neq 0$. However, it can be demonstrated that for this case var $\{X/\theta, H_1\}$ and var $\{Y/\theta, H_1\}$ differ at most by a factor that is proportional to $\bar{q}_{\pm 2M}$. Thus, when M is large enough so that $\bar{q}_{\pm 2M}$ is small, the above conditions will hold, and in fact $E\{[X - E\{X\}][Y - E\{Y\}]/\theta, H_1]$ can be shown to be identically zero.

Observe that the integral in (55) is related to $Q(\cdot, \cdot)$, the tabulated Marcum Q function:

$$\int_0^b v\exp\left\{\frac{v^2+\Omega^2}{-2}\right\}I_0(\Omega v)\,dv=1-Q(\Omega,\,b). \quad (58)$$

Note that $Q(0, b) = e^{-b^2/2}$.

Equation (55) can be expressed in terms of ρ_q ($R_q = 0$ in this subsection because $s_0(t) \equiv 0$), by defining

$$f_1(\rho_q)=\frac{1}{\sqrt{\rho_q}}I_0^{-1}(e^{\rho_q/2}) \quad (59)$$

where $I_0^{-1}(\cdot)$ denotes the inverse modified Bessel function (not the reciprocal $1/I_0(\cdot)$), and ρ_q is given by

$$\rho_q=\frac{1}{\langle N_o\rangle}\int_{T_0}\frac{s_1^2(t)}{q(t)}\,dt.$$

Then

$$P_e=\frac{1}{2}\left[\exp\left\{-\frac{f_1^2(\rho_q)}{2}\right\}+1-Q(\Omega,\,f_1(\rho_q))\right]$$
$$=\frac{1}{2}\left[Q(0,\,f_1(\rho_q))-Q(\Omega,\,f_1(\rho_q))+1\right] \quad (60)$$

where $\Omega^2 = \rho_q$.

The suboptimum detector for (4) and (48) is given by (49) and (50) with $N_o(t)$ replaced by $\langle N_o\rangle$ or equivalently $q(t)$

replaced by 1. Its structure is identical to that shown in Fig. 7 except for replacement of $q(t)$ by 1. Thus the suboptimum detector is a quadrature correlator receiver that generates the statistic $\tilde{p}$ where

$$\tilde{p}^2 = \left[\int_{T_0} \sin \frac{2\pi Mt}{T}\, r(t)\, dt\right]^2 + \left[\int_{T_0} \cos \frac{2\pi Mt}{T}\, r(t)\, dt\right]^2 \triangleq \tilde{y}^2 + \tilde{x}^2. \tag{61}$$

The receiver compares $\tilde{p}^2$ to the threshold $\tilde{\eta}^2$ where $\tilde{\eta}$ is the value of $\tilde{p}$ for which $I_0(A\tilde{p}/\langle N_o\rangle) = \gamma$. (Note that γ is given by (50) with $\lambda = 1$ due to the assumption $P\{H_1\} = 1/2$ and $q(t) = 1$.) The probability of detection error is given by (55) with b replaced by $\tilde{b}$ and Ω^2 replaced by $\tilde{\Omega}^2$, where

$$\tilde{b} = \frac{\tilde{\eta}}{\sqrt{\text{var}\,\{\tilde{X}/\theta, H_1\}}}$$
$$\tilde{\Omega}^2 = \frac{A^2 |T_0|^2}{4\,\text{var}\,\{\tilde{X}/\theta, H_1\}}. \tag{62}$$

Thus

$$\tilde{P}_e = \frac{1}{2}\left[e^{-\tilde{b}^2/2} + 1 - Q(\tilde{\Omega}, \tilde{b})\right] = \frac{1}{2}\left[Q(0, b) - Q(\tilde{\Omega}, \tilde{b}) + 1\right] \tag{63}$$

where as before, $Q(\cdot, \cdot)$ is the tabulated Marcum Q function. In order to derive (63), it has been assumed that $P\{H_1\} = 1/2$, and var $\{\tilde{X}/\theta, H_1\}$ = var $\{\tilde{Y}/\theta, H_1\} \triangleq \sigma_T^2$, and that

$$E\{[\tilde{X} - E\{\tilde{X}/\theta, H_1\}][\tilde{Y} - E\{Y/\theta, H_1\}]/\theta, H_1\} = \frac{\langle N_o\rangle}{2}\int_{T_0} q(t) \sin \frac{4\pi Mt}{T}\, dt \equiv 0. \tag{64}$$

If M is large enough that the sinusoidal term in (64) varies much more rapidly than $q(t)$, then not only is the latter assumption very nearly satisfied, but also since

$$\text{var}\,\{\tilde{X}/\theta, H_1\} = \frac{\langle N_o\rangle}{2}\int_{T_0} q(t)\left[1 + \cos \frac{4\pi Mt}{T}\right] dt$$

and

$$\text{var}\,\{\tilde{Y}/\theta, H_1\} = \frac{\langle N_o\rangle}{2}\int_{T_0} q(t)\left[1 - \cos \frac{4\pi Mt}{T}\right] dt$$

it is clear that the former assumption used in the derivation of (63) is very nearly satisfied. In the specific case when $q(t)$ is given by (21) (after division by $\langle N_o\rangle$), then

$$\int_{T_0} q(t) \sin \frac{4\pi Mt}{T}\, dt = |T_0| b(1-a)\left[\frac{1 - \cos 4\pi Mc}{4\pi M}\right]$$

and

$$\int_{T_0} q(t) \cos \frac{4\pi Mt}{T}\, dt = |T_0| b(1-a) \frac{\sin 4\pi Mc}{4\pi M}.$$

Clearly, whenever c is such that $2Mc$ is an integer, then the above assumptions hold exactly. (Note that this does not confine c to the value 1/2. For instance if $M = 1000$, then c can be as small as 1/2000.) For the case when $q(t)$ is given by (30) (after division by $\langle N_o\rangle$), it is easily demonstrated that

$$\int_{T_0} q(t) \sin \frac{4\pi Mt}{T}\, dt = \int_{T_0} q(t) \cos \frac{4\pi Mt}{T}\, dt \equiv 0$$

hence, the assumptions leading to (63) are valid in this particular case.

Equation (63) can be expressed in terms of ρ ($R = 0$ in this subsection because $s_0(t) \equiv 0$) and the weighted distance between signals, which with $s_0(t) = 0$ becomes

$$d_q = \left[\int_{T_0} s_1^2(t) q(t)\, dt\right]^{1/2}.$$

Thus, defining

$$f_2(\rho) = \sqrt{\frac{d_1^2}{\rho d_q^2}}\, I_0^{-1}(e^{\rho/2})$$

we obtain

$$\tilde{P}_e = \frac{1}{2}\left[\exp\left\{-\frac{f_2^2(\rho)}{2}\right\} + 1 - Q(\Omega, f_2(\rho))\right] \tag{65}$$

where

$$\tilde{\Omega}^2 = \rho \frac{d_1^2}{d_q^2}.$$

In order to be able to compare detector performances, it is necessary to express (60) in terms of ρ rather than ρ_q. Since

$$\rho_q = \frac{(1-R_q)E_q}{(1-R)E}\rho$$

and in this subsection

$$\rho_q = \frac{d_{1/q}^2 \rho}{d_1^2} \tag{66}$$

then (59) becomes

$$f_1(\rho) = \sqrt{\frac{d_1^2}{d_{1/q}^2 \rho}}\, I_0^{-1}\left(\exp\left\{\frac{d_{1/q}^2 \rho}{2d_1^2}\right\}\right). \tag{67}$$

Since $\Omega^2 = \rho_q$, where ρ_q is given by (66) in terms of ρ, P_e given by (60) can now be expressed in terms of ρ. The mathematically complex form of the foregoing equations in which Marcum Q functions and inverses of a Bessel function appear, make it difficult to arrive at a closed form expression for the SNR boost that the suboptimum detector needs in order to achieve a performance level equal to that of the optimum detector. Consequently, two examples are worked out where performance comparisons are investigated for specific mathematical forms of $q(t)$. If approximations to a Bessel function for both small and large arguments are used, it is possible to

obtain approximations to P_e and $\tilde{P}_e$. This is discussed in Appendix A. In Appendix B, bounds on P_e and $\tilde{P}_e$ are presented; however, their usefulness is diminished by the fact that the bounds cannot be used to compare $\tilde{P}_e$ to P_e.

Example 3:

The on–off signaling scheme of Example 1 is reconsidered here assuming that the signals to be detected are given by (48) and the noise obeys the assumptions stated in Example 1 with $c = 1/2$. $f_1(\rho)$ and Ω^2 can be easily expressed in terms of the parameter a (see (67)):

$$f_1(\rho)=\sqrt{\frac{4a}{\rho(1+a)^2}}\, I_0^{-1}\left(\exp\left\{\rho\,\frac{(1+a)^2}{8a}\right\}\right)$$

$$\Omega^2=\rho\,\frac{(1+a)^2}{4a}.$$

Thus, from (60):

$$P_e=\frac{1}{2}\left[\exp\left\{\frac{-2a}{\rho(1+a)^2}\, I_0^{-2}\left(\exp\left\{\rho\,\frac{(1+a)^2}{8a}\right\}\right)\right\}\right.$$

$$+1-Q\left(\sqrt{\rho\,\frac{(1+a)^2}{4a}},\right.$$

$$\left.\left.\sqrt{\frac{4a}{(\rho(1+a)^2}}\, I_0^{-1}\left(\exp\left\{\rho\,\frac{(1+a)^2}{8a}\right\}\right)\right)\right]. \quad (68)$$

It is simple to demonstrate that for this symmetric periodic noise intensity factor $N_0(t)$ (i.e., $c = 1/2$), the assumptions made in the derivation of (55) (i.e., (57)) hold. Furthermore, these assumptions hold for other values of c, $0 < c \leq 1$, as long as $2Mc$ is an integer.

The performance of the suboptimum detector is obtained by evaluating $f_2(\rho)$ and $\tilde{\Omega}$, that is

$$f_2(\rho)=\sqrt{\frac{1}{\rho}}\, I_0^{-1}(e^{\rho/2})$$

$$\tilde{\Omega}^2=\rho$$

so that (see (65))

$$\tilde{P}_e=\frac{1}{2}\left[\exp\left\{-\frac{1}{2\rho}\, I_0^{-2}(e^{\rho/2})\right\}+1\right.$$

$$\left.-Q\left(\sqrt{\rho},\frac{1}{\sqrt{\rho}}\, I_0^{-1}(e^{\rho/2})\right)\right]. \quad (69)$$

The discussion following (64) indicates that the assumptions made in the derivation of $\tilde{P}_e$ are satisfied in this particular example, hence, (69) and (68) can now be compared. Fig. 8 illustrates the differences in performance between the optimum and the suboptimum detectors in terms of the SNR ρ for specific values of the parameter a.

Example 4:

The on–off signaling scheme of Example 1 is reconsidered here assuming that the signals to be detected are given by (48) and the noise obeys the assumptions stated in Example 2. Prior to developing the expressions for P_e and $\tilde{P}_e$, it is worthwhile checking whether or not the assumptions made in deriving P_e and $\tilde{P}_e$ hold. First, the assumption made in (51) is analyzed by evaluating the following integral:

$$\int_{T_0}\frac{s^2(t,\theta)}{q(t)}\,dt=\frac{A^2|T_0|}{2}\left[\frac{1+v^2}{1-v^2}\right][1-(-v)^{2M}\cos 2\theta] \quad (70)$$

where

$$v=\frac{a-1}{1+a+2\sqrt{a}}.$$

Observe that v^2 decreases monotonically from 1 to 0 as a increases from 0 to 1. Thus for $0 < a \leq 1$, $0 \leq v^2 < 1$, implying that $(v^2)^M \ll 1$ for M large enough. Thus, for M such that $v^{2M} \ll 1$, the second term in (70) can be ignored. Second, the requirement var $\{X/\theta, H_1\}$ = var $\{Y/\theta, H_1\}$ is also satisfied for large values of M since

$$\text{var}\,\{X/\theta, H_1\}=\frac{\langle N_o\rangle|T_0|}{2}\left[\frac{1+v^2}{1-v^2}\right][1-(-v)^{2M}]$$

$$\text{var}\,\{Y/\theta, H_1\}=\frac{\langle N_o\rangle|T_0|}{2}\left[\frac{1+v^2}{1-v^2}\right][1+(-v)^{2M}]. \quad (71)$$

The requirement that $E\{[X - E\{X\}][Y - E\{Y\}]/\theta, H_1\} = 0$ can be easily shown to be satisfied exactly. Thus, assuming that M is large enough so that the equations in (71) can be considered to be nearly equal, use of (66) and (67) in (60) yields

$$P_e=\frac{1}{2}\left[\exp\left\{\frac{-\sqrt{a}}{\rho(1+a)}\, I_0^{-2}\left(\exp\left\{\frac{\rho}{2}\,\frac{1+a}{2\sqrt{a}}\right\}\right)\right\}\right.$$

$$+1-Q\left(\sqrt{\frac{\rho(1+a)}{2\sqrt{a}}},\right.$$

$$\left.\left.\sqrt{\frac{2\sqrt{a}}{(1+a)\rho}}\, I_0^{-1}\left(\exp\left\{\frac{\rho}{2}\,\frac{1+a}{2\sqrt{a}}\right\}\right)\right)\right]. \quad (72)$$

The assumptions made in the derivation of (63) hold here as demonstrated in the discussion following (64). Furthermore, since

$$f_2(\rho)=\sqrt{\frac{1}{\rho}}\, I_0^{-1}(e^{\rho/2})$$

and $\tilde{\Omega}^2 = \rho$, it is clear (see equations preceding (69)) that the expression for $\tilde{P}_e$ in this particular example is identical to that derived for Example 3 (see (69)). In Fig. 9 graphs of P_e and $\tilde{P}_e$ are presented in terms of the SNR ρ for specific values of the parameter a, thus illustrating differences in performance between the optimum and suboptimum detectors for the signal specified in (48).

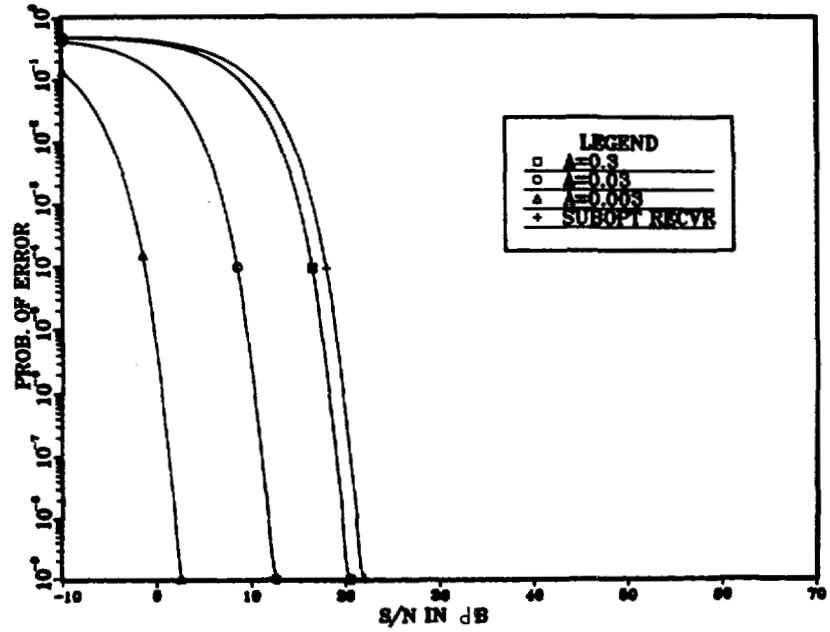

Fig. 8. Receiver performance for Example 3.

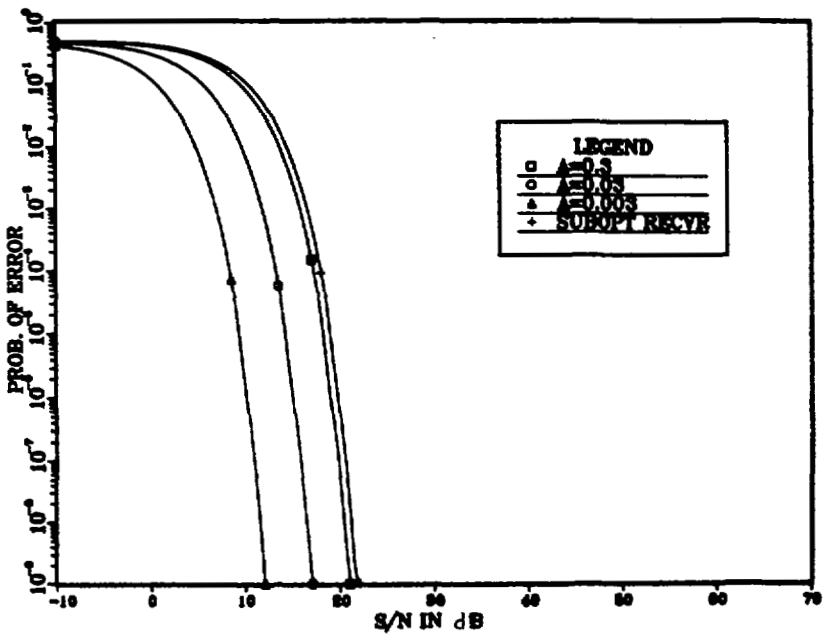

Fig. 9. Receiver performance for Example 4.

IV. Detection of a Sinusoid with Random Amplitude and Phase

The signal detection problem addressed in this section is modeled in the conventional way as a hypothesis testing problem (see (4)) with

$$s_1(t) = \mathcal{A}s(t,\theta) = \mathcal{A}\sin\left(\frac{2\pi Mt}{T}+\theta\right)$$
$$s_0(t) \equiv 0 \tag{73}$$

where θ is a uniformly distributed random variable over $[0, 2\pi]$, and $\mathcal{A}$ is a Rayleigh random variable (independent of θ), with

$$p_{\mathcal{A}}(A) = \frac{A}{A_0^2}\, e^{-A^2/2A_0} u(A). \tag{74}$$

The optimum detector for (4) (with modifications given by (73) and (74)) is given by (8) with [9, p. 206]

$$Z[\{r(t)\}] = \frac{1}{2\pi}\int_0^{2\pi}\int_{-\infty}^{\infty} \exp\left\{\frac{1}{\langle N_o\rangle} \cdot \int_{T_0}\frac{As(t,\alpha)}{q(t)}\, r(t)\, dt\right\} p_{\mathcal{A}}(A)\, dA\, d\alpha \tag{75}$$

$$\gamma = \lambda \exp\left\{\frac{1}{2\langle N_o\rangle}\int_{-\infty}^{\infty}\int_{T_0}\frac{As^2(t,\alpha)}{q(t)}\, dt p_{\mathcal{A}}(A)\, dA\right\}. \tag{76}$$

The structure of this receiver is shown in Fig. 10.

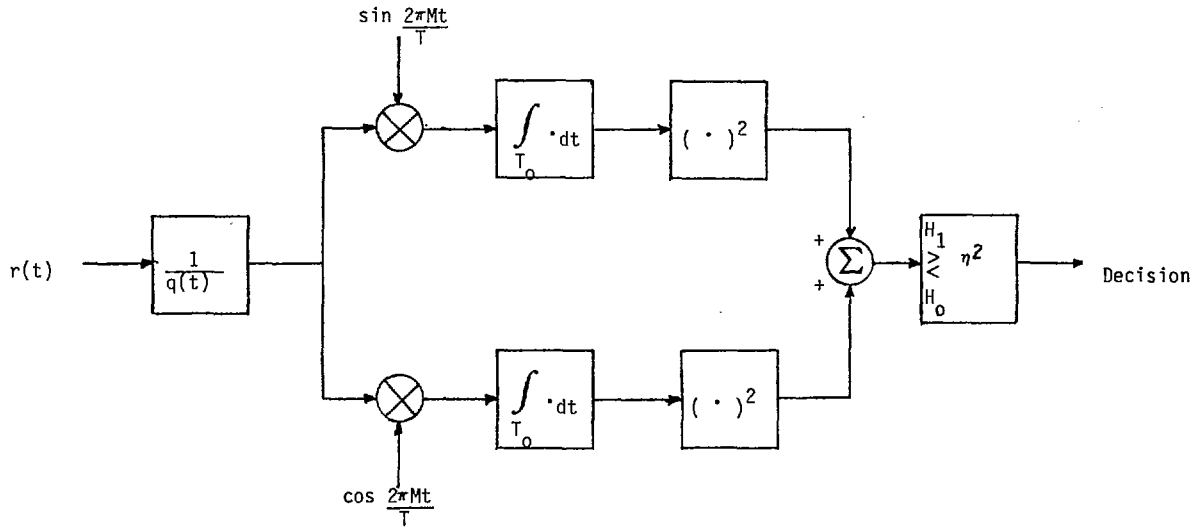

Fig. 10. Optimum receiver for sinusoidal signals having random amplitude and random phase.

Derivation of (75) and (76) is based on the assumption that $T_0 \gg T$ so that the integral

$$\int_{T_0} \frac{s^2(t,\theta)}{q(t)}\,dt \triangleq K \tag{77}$$

is not a function of θ. This type of assumption was stated in (51), and investigated for two different functional forms for $q(t)$. Observe that if the conditions stated in (52) are satisfied, then (77) is independent of θ regardless of the length T_0. A more compact notation for (73) is possible using the quantity p defined by (54). Observing that (75) is just (49) integrated over the pdf of $\mathfrak{A}$, it is simple to show that

$$Z[\{r(t)\}] = \exp\left\{\frac{p^2 A_0^2}{2(K\langle N_o\rangle A_0^2 + \langle N_o\rangle^2)}\right\} \tag{78}$$

$$\gamma = \lambda\,\frac{\langle N_o\rangle + A_0^2 K}{\langle N_o\rangle} \tag{79}$$

where K is given by (77). Performance evaluation for this detector is based on identical assumptions made in the derivation of P_e in the previous section (with A fixed). In order to express P_e as a function of SNR, we must realize that since the amplitude of the sinusoid is random, the SNR is random. We define an average SNR, using the definition of SNR and (74). We obtain

$$E\{\rho\} = \bar{\rho} = \int_{-\infty}^{\infty} \rho(A)\,p_{\mathfrak{A}}(A)\,dA = \frac{|T_0|A_0^2}{\langle N_o\rangle} \tag{80}$$

and assuming again $P\{H_1\} = 1/2$

$$P_e = \frac{1}{2}\left\{\left[\frac{1}{1+2K\bar{\rho}/|T_0|}\right]^{[1+|T_0|/2K\bar{\rho}]} + 1 - \left[\frac{1}{1+2K\bar{\rho}/|T_0|}\right]^{|T_0|/2K\rho}\right\}. \tag{81}$$

Defining

$$\mu = \frac{2K\bar{\rho}}{|T_0|}$$

we can express (81) as

$$P_e = \frac{1}{2}\left[\left(1 - \frac{1}{1+1/\mu}\right)\left(\frac{1}{1+\mu}\right)^{1/\mu}\right]$$

and for large values of μ (i.e., large SNR)

$$P_e \simeq \frac{1}{2}\left[1 - \left(\frac{1}{\Omega}\right)^{1/\Omega}\right].$$

This shows that the performance of this quadrature correlator receiver essentially depends on the inverse of the average SNR, whereas in the two previous sections, the detector performance depends on SNR exponentially. The suboptimum detector for (4) (with modification given by (73) and (74)) is also a quadrature correlator receiver given by (75) and (76), with $q(t)$ replaced by 1. The structure of this receiver is identical to that shown in Fig. 10 except for replacement of $q(t)$ by 1. An expression similar to (78) can be derived for this receiver and is identical to (78) in form except that in place of p, we have $\tilde{p}$ given by (61) and K is replaced with $\tilde{K}$ where $\tilde{K}$ is given by (77) with $q(t) = 1$. Performance evaluation for this suboptimum detector is based on identical assumptions made in the derivation of $\tilde{P}_e$ in the previous section (with A fixed). We obtain as a function of $\bar{\rho}$

$$\tilde{P}_e = \frac{1}{2}\exp\left\{\frac{|T_0|\langle N_o\rangle}{2\tilde{\sigma}_T^2} - \frac{(\bar{\rho}+1)}{\bar{\rho}}\ln\frac{1}{\bar{\rho}+1}\right\} + 1 - \exp\left\{\frac{\bar{\rho}+1}{(2\tilde{\sigma}_T^2/|T_0|\langle N_o\rangle + \bar{\rho})\bar{\rho}}\ln\frac{1}{\bar{\rho}+1}\right\} \tag{82}$$

where

$$\tilde{\sigma}_T^2 = \operatorname{var}\{\tilde{X}/\theta, H_1\}. \tag{83}$$

Evaluation of P_e and $\tilde{P}_e$ requires specific assumptions about the noise periodic factor $N_o(t)$.

Example 5:

The on–off signaling scheme of Example 1 is reconsidered here assuming that the signals to be detected are given by (73) (with added constraint given by (74)), and the noise obeys the assumptions stated in Example 1 with $c = 1/2$. It is simple to demonstrate here that K (see (77)) is not a function of θ. Furthermore, (81) becomes

$$P_e=\frac{1}{2}\left\{\left[\frac{1}{1+\dfrac{(1+a)^2}{4a}\bar{\rho}}\right]^{[1+4a/(1+a^2)\bar{\rho}]} +1-\left[\frac{1}{1+\dfrac{(1+a)^2}{4a}\bar{\rho}}\right]^{4a/(1+a)2\bar{\rho}}\right\}.$$

Also, using (82) and (83), the performance of the suboptimum detector becomes

$$\tilde{P}_e=\frac{1}{2}\left\{\left[\frac{1}{\bar{\rho}+1}\right]^{(\bar{\rho}+1)/\bar{\rho}}+1-\left[\frac{1}{\bar{\rho}+1}\right]^{1/\bar{\rho}}\right\}. \quad (84)$$

When the same on–off signaling scheme is used in the presence of noise with characteristics given in Example 2, the performance of the suboptimum detector is identical to that when the noise obeys the assumptions stated in Example 1. Hence, (84) specifies the performance of this suboptimum detector. The optimum detector has performance given by

$$P_e=\frac{1}{2}\left\{\left[\frac{1}{1+\dfrac{1+a}{2\sqrt{a}}\bar{\rho}}\right]^{[1+2\sqrt{a}/(1+a)\bar{\rho}]} +1-\left[\frac{1}{1+\dfrac{1+a}{2\sqrt{a}}\bar{\rho}}\right]^{2\sqrt{a}/(1+a)\bar{\rho}}\right\}. \quad (85)$$

Performance comparisons for these detectors are shown in Figs. 11 and 12.

V. Discussion of Results

The mathematical results as well as the graphs shown for the specific examples considered reveal several items of interest which are now discussed.

The behavior of detector probability of error as a function of SNR is similar to that encountered when the additive noise is stationary white Gaussian. That is, the decay in probability of error for the detector of sure signals and of a sinusoid with random phase, as a function of SNR is exponential. For the detection of a sinusoid having random amplitude and phase, probability of error decays only as the inverse of SNR. These observations are not surprising for the optimum detectors presented because these structures stationarize the noise as part of the processing of the received signal. It is somewhat surprising, however, that the above observations are valid for the suboptimum detectors under consideration. Closer scrutiny of (for example) (18), reveals, however, that the observed behavior of suboptimum detectors as a function of SNR does not always occur. In (18), $\tilde{P}_e$ depends on SNR and on the parameter J. If $J = 1$ (as is the case in all examples presented) we have the typical exponential drop of error probability as a function of SNR. If, however, $J \gg 1$ (which could occur for instance if $[s_1(t) - s_0(t)]^2$ and $q(t)$ are highly "correlated"), then the decay of $\tilde{P}_e$ as a function of SNR becomes much slower.

It is well known that detectors for sure signals and detectors for sinusoidal signals with random phase can be made to operate equally by increasing the input SNR to the latter by an appropriate amount. When P_e is large ($0.05 \lesssim P_e \lesssim 0.5$), the latter detector requires approximately 3 dB higher input SNR than the former detector. For small values of P_e ($P_e < 10^{-4}$), the two detectors operate equally with about the same input SNR. Put differently, at high input SNR's, the lack of phase knowledge affects the optimum detector performance negligibly. Figs. 1 and 7 show that the same statement holds true for detection in additive cyclostationary white noise. This is not surprising given the facts highlighted in the previous paragraph. For instance, looking at Figs. 3 and 9, we see about a 2.5-dB-input SNR difference between the optimum detectors at $P_e = 10^{-1}$ and about 0.5-dB input SNR difference at $P_e = 10^{-6}$.

The performance of the suboptimum detector can sometimes be comparable to that of its optimum counterpart. Depending upon the problem under consideration, the difference in performance between the two detectors can be negligible. For such cases, nothing is to be gained by building an optimum synchronized detector. However, before deciding whether an optimum (synchronized) or a suboptimum (unsynchronized) detector is to be built, full knowledge of the $q(t)$ function is required because, as the results demonstrate, detector performance is not only dependent on noise strength, but also noise "shape" (i.e., $q(t)$). As demonstrated by (19), the parameter D can be used to determine, for sure signal detection problems, the level of suboptimality of the unsynchronized detector in terms of input SNR. Furthermore, if an optimum detector is to be built, ability to properly synchronize it must be fully accounted for. As Example 1 (continued) demonstrates, an optimum detector that is improperly synchronized can exhibit a performance (in terms of P_e as a function of input SNR) that is comparable or worse than the suboptimum detector that requires no synchronization. (See also Fig. 6). It is therefore apparent that the added complexity of building an optimum detector might yield very little in return (in terms of performance) if synchronization cannot be adequately maintained.

It is apparent from Figs. 4, 9, and 12 that the level of suboptimality exhibited by the suboptimum detector decreases as the "randomness" in the signal to be detected increases. That is, as the number of random parameters in the signal increases, the difference in performance between the optimum and its corresponding suboptimum detector at fixed SNR

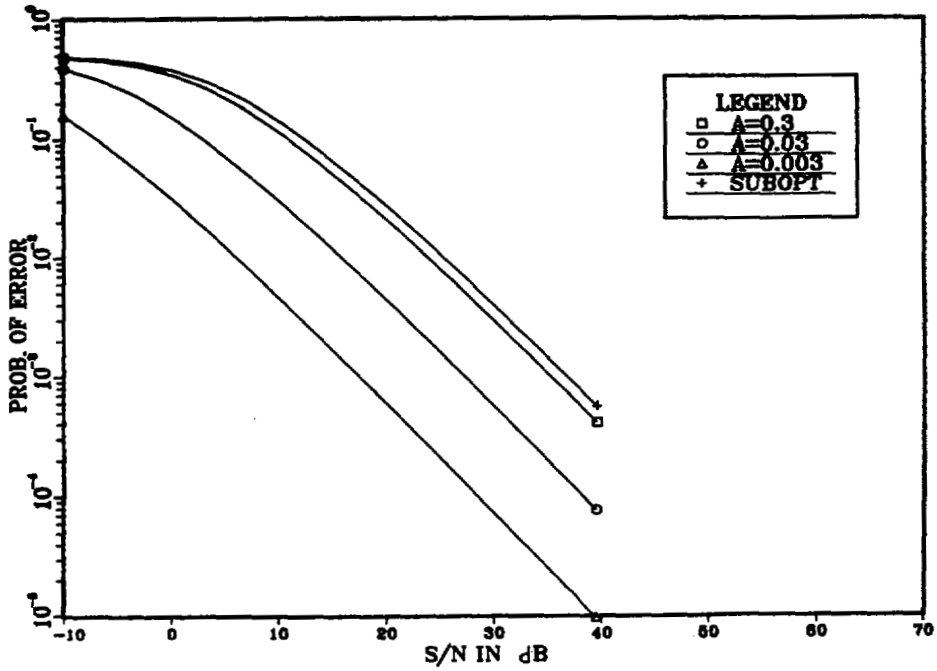

Fig. 11. Receiver performance for Example 5 with a symmetric noise intensity factor given in Example 1.

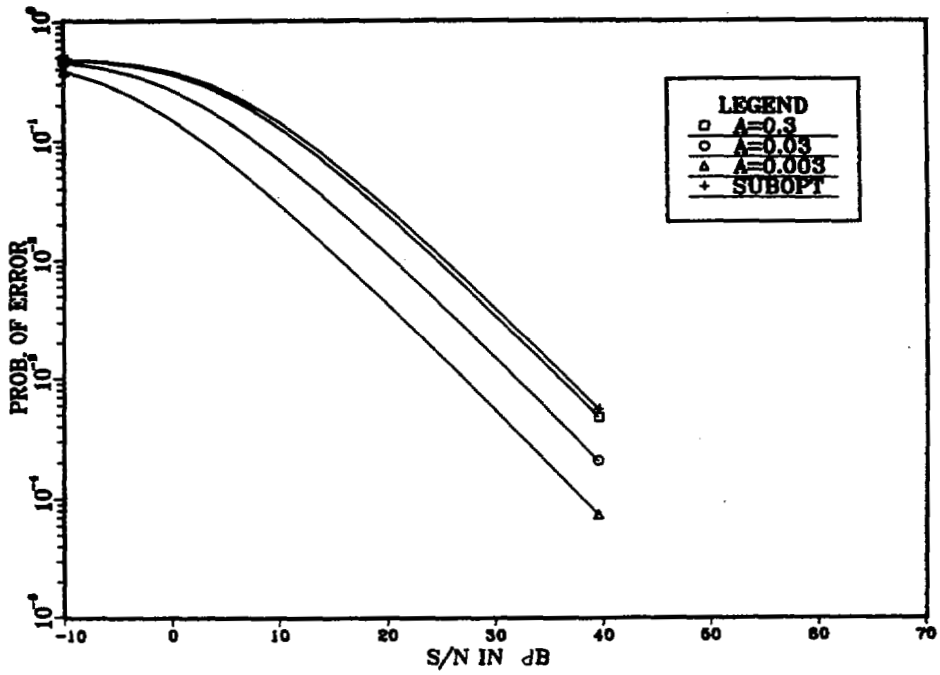

Fig. 12. Receiver performance for Example 5 with noise intensity factor given in Example 2.

decreases. This result is to be expected since the optimum detector is synchronized to the noise only. As the signal randomness increases (i.e., as phase or amplitude and phase become random), the optimum detector is less able to exploit low-noise intervals because it does not have as much information about the signal in those low-noise intervals. Note also that the rate at which the optimum detection problem becomes singular (as the parameter a in the examples approaches zero, meaning that the noise intensity approaches zero over specific time spans) decreases as the signal randomness increases. This is to be expected in light of the aforementioned situation of the optimum detector's being less able to exploit low-noise intervals as the signal randomness increases. A similar observation involving optimum and suboptimum detector analyses and comparisons has been reported in [10]. The authors study the problem of detecting a Gaussian process (propagating underwater) by a sensor array that is steered on target. Assuming long observation times, low SNR conditions, and equal SNR at each sensor, they show that the optimum detector must add all signals collected by the sensors and

process them with a filter-squarer-integrator (FSI) receiver. The performance of this receiver is not specified in terms of probability of error, but rather in terms of SNR at the output of the detector. When the SNR is not the same at each sensor, the FSI receiver is proposed and studied as a suboptimum detector. The optimum detector for the case in which the SNR is not the same at each sensor is still a summer followed by an FSI receiver, but prior to summing, channel noise equalization (which requires noise synchronization in the spatial dimension) is necessary by attenuating noisy channels and amplifying quiet ones. That is, a synchronized detector can vastly outperform an unsynchronized detector, when the noise intensity shows strong variations that bring the noise intensity to very low levels over nonnegligible intervals of time. The authors of [10] analyze other suboptimum detection schemes in which they show that small performance loss can be achieved with substantial system simplification when filtering operations in the FSI receiver are simplified or eliminated.

VI. Conclusions

In this paper, optimum and suboptimum receivers for detecting sure signals, sinusoids with random phase, and sinusoids with random amplitude and phase in additive white Gaussian nonstationary noise are analyzed. Suboptimum detectors are designed according to a specific methodology, as described in Section I. The performance of these suboptimum detectors is compared to their optimum counterparts, which, as shown in Sections II, III, and IV, are very similar in structure to conventional detectors for signals in additive stationary WGN, except that a noise stationarization operation precedes the optimum detectors. It is demonstrated that performance differences between optimum and suboptimum detectors can be negligible but also can be substantial. These differences in performance are a function of the signal being detected and the intensity time-variations exhibited by the nonstationary noise. In cases of negligible performance difference, nothing is gained by implementing the (more complex) optimum detector that must be synchronized to the noise intensity variations. In fact, it is demonstrated in Section II that an improperly synchronized (otherwise optimum) detector, can exhibit inferior performance compared with the corresponding suboptimum detector that does not require synchronization. The methodology developed for analyzing detection problems for known or partially known signals, is applicable not just to cyclostationary noise, but also to other nonstationary white Gaussian noises.

Appendix A

Approximations to P_e Derived in Section III

From Section III (equation (60)) we have the closed-form expression for P_e, namely

$$P_e=\frac{1}{2}\left[\exp\left\{-\frac{f_1^2(\rho)}{2}\right\}+\int_{f1(\rho)}^{\infty} v\exp\left\{-\frac{v^2+\Omega^2}{2}\right\} I_0(\Omega v)\,dv\right] \quad \text{(A1)}$$

where (see (67))

$$f_1(\rho)=\sqrt{\frac{d_1^2}{d_{1/q}^2\rho}}\, I_0^{-1}\left(\exp\left\{\frac{d_{1/q}^2\rho}{2d_1^2}\right\}\right) \quad \text{(A2)}$$

$$\Omega^2=\frac{d_{1/q}^2\rho}{d_1^2}. \quad \text{(A3)}$$

Since for $x \gg 1$

$$I_0(x)\simeq\frac{e^x}{\sqrt{2\pi x}} \quad \text{(A4)}$$

we see that

$$I_0^{-1}\left(\exp\left\{\frac{d_{1/q}^2\rho}{2d_1^2}\right\}\right)\simeq\frac{d_{1/q}^2\rho}{2d_1^2} \quad \text{(A5)}$$

if $d_{1/q}^2\rho/2d_1^2$ is large. (Observe that if we are attempting to obtain $I_0^{-1}(e^y)$ where y is large, then, we must solve the nonlinear equation

$$e^y\simeq\frac{e^x}{\sqrt{2\pi x}} \Rightarrow x-\frac{1}{2}\ln 2\pi x\simeq y.$$

If for instance $y = 20$, then $x \simeq 22.5$ and we see that $x \simeq y$ (i.e., we commit a 12-percent error here by approximating x by y).

Thus for $d_{1/q}^2\rho/2d_1^2$ large

$$f_1(\rho)\simeq\sqrt{\frac{d_{1/q}^2\rho}{4d_1^2}}. \quad \text{(A6)}$$

Observe furthermore that

$$f_1(\rho)\Omega\simeq\frac{d_{1/q}^2\rho}{2d_1^2}\gg 1 \quad \text{(A7)}$$

so that the argument of the Bessel function appearing in (A1) is always large so that use of (A4) can now be made. We obtain

$$P_e\simeq\frac{1}{2}\left[\exp\left\{-\frac{f_1^2(\rho)}{2}\right\}+\int_{f_1(\rho)}^{\infty}\sqrt{v}e^{-(v-\Omega)^2/2}\frac{dv}{\sqrt{2\pi\Omega}}\right].$$

For $f_1(\rho)$ large, the dominant term in the integrand is the exponential so that the behavior of the "tails" of the integrand is very much like that of a Gaussian density of unit variance. Thus

$$P_e\simeq\frac{1}{2}\left[\exp\left\{-\frac{f_1^2(\rho)}{2}\right\}+\frac{1}{\sqrt{\Omega}}\int_{f_1(\rho)-\Omega}^{\infty}\frac{1}{\sqrt{2\pi}}e^{-z^2/2}\,dz\right]$$

and using (A3) as well as (A6), we obtain

$$P_e\simeq\frac{1}{2}\left[\exp\left\{-\frac{d_{1/q}^2\rho}{8d_1^2}\right\}+\left(\frac{d_1^2}{d_{1/q}^2\rho}\right)^{1/4}\cdot\left\{1-\operatorname{erfc}\left(\frac{1}{2}\sqrt{\frac{d_{1/q}^2\rho}{d_1^2}}\right)\right\}\right]. \quad \text{(A8)}$$

It must be pointed out that the ratio $d_{1/q}^2\rho/d_1^2$ can be large even though ρ is not large. For instance, if one uses the results of Example 3, it is found that

$$\frac{d_{1/q}^2}{d_1^2}\rho=\frac{(a+1)^2}{4a}\rho$$

so that for small values of a, the ratio can be very large. (For $\rho = 0.1$ and $a = 0.003$, this ratio equals 8.38.)

Similar analysis can be applied to $\tilde{P}_e$, where $\tilde{P}_e$ is given by (A1) with $f_1(\rho)$ replaced by $f_2(\rho)$ and Ω replaced by $\tilde{\Omega}$, where

$$f_2(\rho)=\sqrt{\frac{d_1^2}{\rho d_q^2}}\,I_0^{-1}(e^{\rho/2}) \tag{A9}$$

$$\tilde{\Omega}^2=\frac{d_1^2}{d_q^2}\rho. \tag{A10}$$

If ρ is very large, then $I_0^{-1}(e^{\rho/2}) \simeq \rho/2$ and

$$f_2(\rho)\simeq\sqrt{\frac{d_1^2\rho}{4d_q^2}}. \tag{A11}$$

Furthermore

$$f_2(\rho)\tilde{\Omega}=\frac{d_1^2\rho}{4d_q^2} \tag{A12}$$

so that if ρ is large enough to guarantee that

$$\frac{d_1^2\rho}{2d_q^2}\gg 1$$

then the argument of the Bessel function appearing in the equation for P_e is always large so that use of (A4) yields

$$\tilde{P}_e\simeq\frac{1}{2}\left[\exp\left\{-\frac{f_2^2(\rho)}{2}\right\}+\int_{f_2(\rho)}^{\infty}\sqrt{v}e^{-(v-\tilde{\Omega})^2/2}\,\frac{dv}{\sqrt{2\pi\tilde{\Omega}}}\right].$$

Using similar arguments to those used in the development of (A8), we have

$$\tilde{P}_e\simeq\frac{1}{2}\left[\exp\left\{-\frac{d_1^2\rho}{8d_q^2}\right\}+\left(\frac{d_q^2}{d_1^2\rho}\right)^{1/4}\cdot\left\{1-\operatorname{erfc}\left(\frac{1}{2}\sqrt{\frac{d_1^2\rho}{d_q^2}}\right)\right\}\right]. \tag{A13}$$

Using the approximations (A8) and (A13), it appears that $P_e \simeq \tilde{P}_e$ provided that

$$\frac{d_1^2}{d_{1/q}^2\rho_o}=\frac{d_q^2}{d_1^2\rho_{so}} \tag{A14}$$

where the SNR boost D, that is

$$D=\frac{\rho_{so}}{\rho_o}$$

is the amount by which the SNR for the suboptimum receiver must be increased for it to have the same performance as the optimum receiver. Clearly, from (A14),

$$D=\frac{d_{1/q}^2 d_q^2}{d_1^4} \tag{A15}$$

and using the CBS inequality, it is simple to show that $D \geq 1$. Furthermore (A15) is identical to the SNR boost result for the problem discussed in Section II.

The results of Example 3 yield

$$D=\frac{(a+1)^2}{4a}\in[1,\infty]$$

so that large SNR boosts are required when the parameter a is small. This result however is valid only for large SNR.

Another type of approximation is possible using

$$I_0(x)\simeq 1+(x/2)^2 \tag{A16}$$

which is valid for small values of x (typically $0 \leq x < 1.4$). Returning to (A2) and assuming that

$$\frac{d_{1/q}^2\rho}{2d_1^2}\ll 1 \tag{A17}$$

then

$$I_0^{-1}\left(\exp\left\{\frac{d_{1/q}^2\rho}{2d_1^2}\right\}\right)\simeq 2\sqrt{\exp\left\{\frac{d_{1/q}^2\rho}{2d_1^2}\right\}-1}\simeq 2\sqrt{\frac{d_{1/q}^2\rho}{2d_1^2}}. \tag{A18}$$

In (A18) we have further used the approximation $e^y \simeq 1 + y$ for $y \ll 1$. Thus

$$f_1(\rho)\simeq\sqrt{\frac{d_1^2}{d_{1/q}^2\rho}}\sqrt{\frac{2d_{1/q}^2\rho}{d_1^2}}=\sqrt{2} \tag{A19}$$

and furthermore

$$f_1(\rho)\Omega\simeq\sqrt{\frac{2d_{1/q}^2\rho}{d_1^2}}$$

is small also due to the assumption of equation (A17). Since (A1) can be expressed in the form

$$P_e=\frac{1}{2}\left[\exp\left\{-\frac{f_1^2(\rho)}{2}+1-\int_0^{f_1(\rho)}v\exp\left\{-\frac{v^2+\Omega^2}{2}\right\}I_0(\Omega v)\,dv\right]\right.$$

we can instead work with an approximation of this expression,

namely

$$P_e \simeq \frac{1}{2}\left[\exp\left\{-\frac{f_1^2(\rho)}{2}\right\}+1 - \int_0^{f_1(\rho)} v \exp\left\{-\frac{v^2+\Omega^2}{2}\right\}\left[1+\left(\frac{\Omega v}{2}\right)^2\right] dv\right]$$

$$= \frac{1}{2}\left[\exp\left\{-\frac{f_1^2(\rho)}{2}\right\}+1-e^{-\Omega^2/2}\left\{1-e^{-f_1^2(\rho)/2} - \frac{\Omega^2}{2}\left\langle e^{-f_1^2(\rho)/2}\left(\frac{f_1^2(\rho)}{2}+1\right)-1\right\rangle\right\}\right].$$

Using (A18), we obtain the approximation

$$P_e \simeq \frac{1}{2}\left[e^{-1}+1-e^{-\Omega^2/2}\left\{1-e^{-1}-\frac{\Omega^2}{2}\langle 2e^{-1}-1\rangle\right\}\right]$$

where from (A3)

$$\frac{\Omega^2}{2} = \frac{d_{1/q}^2 \rho}{2d_1^2}.$$

It can thus be concluded that for $\Omega^2/2 \ll 1$

$$P_e \simeq \frac{1}{2}\left[1.37 - e^{-\Omega^2/2}\left\{0.63+0.26\frac{\Omega^2}{2}\right\}\right].$$

Similar analysis applied to $\tilde{P}_e$, assuming $\rho \ll 1$, yields (from (A9))

$$f_2(\rho) \simeq \sqrt{\frac{d_1^2}{\rho d_q^2}}\, 2\sqrt{\exp\left(\frac{\rho}{2}\right)-1} \simeq \sqrt{\frac{2d_1^2}{d_q^2}}. \quad \text{(A20)}$$

Furthermore

$$f_2(\rho)\tilde{\Omega} = \frac{d_1^2 \rho}{2d_q^2} \quad \text{(A21)}$$

so that if ρ is small enough for the ratio in (A21) to be small, then

$$\tilde{P}_e = \frac{1}{2}\left[e^{-f_2^2(\rho)/2}+1-\int_0^{f_2(\rho)} v \exp\left\{-\frac{v^2+\tilde{\Omega}^2}{2}\right\} I_0(\tilde{\Omega}v)\, dv\right]$$

$$\simeq \frac{1}{2}\left[e^{-f_2^2(\rho)/2}+1-\int_0^{f_2(\rho)} v \exp\left\{-\frac{v^2+\tilde{\Omega}^2}{2}\right\} \cdot \left\langle 1+\left(\frac{\tilde{\Omega}v}{2}\right)^2\right\rangle dv\right]$$

$$= \frac{1}{2}\left[e^{-f_2^2(\rho)/2}+1-e^{-\tilde{\Omega}^2/2}\left\{1-e^{-f_2^2(\rho)/2}-\frac{\tilde{\Omega}^2}{2} \cdot \left\langle e^{-f_2^2(\rho)/2}\left(\frac{f_2^2(\rho)}{2}+1\right)-1\right\rangle\right\}\right].$$

Thus

$$P_e \simeq \frac{1}{2}\left[\exp\left\{-\frac{d_1^2}{d_q^2}\right\}+1-e^{-\tilde{\Omega}^2/2}\left\{1-\exp\left\{-\frac{d_1^2}{d_q^2}\right\} - \frac{\tilde{\Omega}^2}{2}\left\langle \exp\left\{-\frac{d_1^2}{d_q^2}\right\}\left(\frac{d_1^2}{d_q^2}+1\right)-1\right\rangle\right\}\right].$$

If we assume $d_1^2/d_q^2 \simeq 1$ (this would allow one to only require small SNR ρ in the foregoing analysis), so that

$$\tilde{P}_e \simeq \frac{1}{2}\left[e^{-1}+1-e^{-\tilde{\Omega}^2/2}\left\{1-e^{-1}-\frac{\tilde{\Omega}^2}{2}\langle 2e^{-1}-1\rangle\right\}\right]. \quad \text{(A22)}$$

Observe from the results of Example 3 that $d_1^2/d_q^2 = 1$. This latest assumption is therefore not unreasonable, and, furthermore, it shows that $\tilde{P}_e \simeq P_e$ if $\Omega^2 = \tilde{\Omega}^2$ or equivalently, if

$$\frac{d_{1/q}^2 \rho_o}{d_1^2} = \frac{d_1^2}{d_q^2}\rho_{so}. \quad \text{(A23)}$$

From (A23) we once again obtain the SNR boost factor D, namely

$$D = \frac{\rho_{so}}{\rho_o} = \frac{d_{1/q}^2 d_q^2}{d_1^4} \geq 1.$$

Using once again the results of Example 3, we obtain

$$D = \frac{(a+1)^2}{4a}$$

as before, and it is valid for small values of SNR as well.

Appendix B

Bounds on P_e and $\tilde{P}_e$ Derived in Section III

From Section III, both P_e and $\tilde{P}_e$ take on the general form

$$P\{\text{error}\} = \frac{1}{2}\left[e^{-b^2/2} + \int_b^\infty v \exp\left\{-\frac{v^2+\Omega^2}{2}\right\} I_0(\Omega v)\, dv\right].$$

Since $I_0(x)$ is a monotonic increasing function, we have

$$\int_b^\infty v \exp\left\{-\frac{v^2+\Omega^2}{2}\right\} I_0(\Omega v)\, dv \geq \int_b^\infty v \exp\left\{-\frac{v^2+\Omega^2}{2}\right\} dv I_0(\Omega b)$$

and this last integral becomes $e^{-\Omega^2/2}e^{-b^2/2}$, so that

$$P\{\text{error}\} \geq \frac{1}{2}\left[e^{-b^2/2}+e^{-\Omega^2/2}e^{-b^2/2}I_0(\Omega b)\right]$$

$$= \frac{1}{2}\left[e^{-b^2/2}(1+e^{-\Omega^2/2}I_0(\Omega b)\right].$$

Furthermore

$$P\{\text{error}\} = \frac{1}{2}\left[e^{-b^2/2} + 1 - \int_0^b v \exp\left\{-\frac{v^2+\Omega^2}{2}\right\} I_0(\Omega v)\, dv\right]$$

and because $I_0(0) = 1$, we have

$$\int_0^b v \exp\left\{-\frac{v^2+\Omega^2}{2}\right\} I_0(\Omega v)\, dv \geq \int_0^b v \exp\left\{-\frac{v^2+\Omega^2}{2}\right\} dv.$$

Thus

$$P\{\text{error}\} \leq \frac{1}{2}\left[e^{-b^2/2} + 1 - \int_0^b v \exp\left\{-\frac{v^2+\Omega^2}{2}\right\} dv\right]$$

$$= \frac{1}{2}\left[e^{-b^2/2} + 1 - e^{-\Omega^2/2}(1 - e^{-b^2/2})\right]$$

$$= \frac{1}{2}\left[e^{-b^2/2}(1 + e^{-\Omega^2/2}) + (1 - e^{-\Omega^2/2})\right].$$

Observe that this last upper bound becomes useless for

$$b \leq \left[2 \ln \frac{1}{\tanh(\Omega^2/4)}\right]^{1/2}.$$

It turns out that the above lower bound on $P\{\text{error}\}$ takes on a particularly simple form when applied to P_e. From (A2) and (A3)

$$f_1(\rho)\Omega = I_0^{-1}\left(\exp\left\{\frac{d_{1/q}^2 \rho}{2d_1^2}\right\}\right)$$

so that

$$I_0(f_1(\rho)\Omega) = \exp\left\{\frac{d_{1/q}^2 \rho}{2d_1^2}\right\}$$

and

$$P_e \geq \frac{1}{2}\left[e^{-f_1^2(\rho)/2}(1 + e^{-\Omega^2/2} e^{-\Omega^2/2})\right]$$

$$= \frac{1}{2} e^{-f_1^2(\rho)/2}(1 + e^{-\Omega^2}).$$

Acknowledgment

The author acknowledges Prof. W. A. Gardner of the University of California, Davis, for formulating the detection performance/comparison problem addressed in this paper, for proposing the noise-stationarizing approach to the solution, and for assisting with the presentation of the results.

References

[1] H. L. Van Trees, *Detection, Estimation, and Modulation Theory, Part I.* New York: Wiley, 1968.
[2] L. E. Franks, *Signal Theory.* Englewood Cliffs, NJ: Prentice-Hall, 1969, ch. 8.
[3] W. A. Gardner, *Introduction to Random Processes with Applications to Signals and Systems.* New York: Macmillan, 1985.
[4] L. J. Ziomek, *Underwater Acoustics.* New York: Academic, 1985.
[5] W. A. Gardner, "Stationarizable random processes," *IEEE Trans. Inform. Theory*, vol. IT-24, pp. 8–22, 1978.
[6] H. L. Hurd, "Stationarizing properties of random shifts," *SIAM J. Applied Math.*, vol. 26, pp. 203–212, 1974.
[7] W. A. Gardner, "Structural characterization of locally optimum detectors in terms of locally optimum estimators and correlators," *IEEE Trans. Inform. Theory*, vol. IT-28, pp. 924–932, 1982.
[8] Paul Penfield, Jr., "Fourier coefficients of power-law devices," *J. Franklin Inst.*, vol. 139, pp. 107–122, Feb. 1972.
[9] A. D. Whalen, *Detection of Signals in Noise.* New York: Academic, 1971, ch. 7.
[10] P. M. Schultheiss and F. B. Tuteur, "Optimum and sub-optimum detection of directional Gaussian signals in an isotropic Gaussian noise field, Part 1: Likelihood ratio and power detectors," *IEEE Trans. Mil. Electron.*, vol. ME-20, pp. 197–202, 1965.

★

Daniel Bukofzer (S'78–M'79) received the B.S. degree from California State University, Los Angeles, in 1970, the M.S. degree from the University of California, Los Angeles, in 1972, and the Ph.D. degree from the University of California, Davis, in 1979, all in engineering.

During 1972–1973, he was a member of the Technical Staff at Bell Telephone Laboratories in Holmdel, NJ. Since 1980 he has been on the faculty of the Electrical and Computer Engineering Department at the Naval Postgraduate School, Monterey, CA, and since 1974 has also been affiliated with the Electronics Engineering Department at the Lawrence Livermore National Laboratory, Livermore, CA. His research interests involve signal detection and estimation problems, and efficient modulation/coding techniques for digital communication applications.

Dr. Bukofzer is a member of Tau Beta Pi, Eta Kappa Nu, Phi Kappa Phi, and Sigma Xi.